Macromolecules
ARTICLE

Macromolecules **2011**, *44*, 1053–1061 **1053**
DOI: 10.1021/ma1022567

A Multiscale Modeling Protocol To Generate Realistic Polymer Surfaces

Jan-Willem Handgraaf,*,† Ruben Serral Gracia,† Shyamal K. Nath,‡ Zhong Chen,§ Shih-Hung Chou,§ Richard B. Ross,§ Nate E. Schultz,§ and Johannes G. E. M. Fraaije†,⊥

†*Culgi B.V., P.O. Box 252, 2300 AG Leiden, The Netherlands,* ‡*Culgi Inc., Albuquerque, New Mexico 87113, United States,* §*3M Company, St. Paul, Minnesota 55144-1000, United States, and* ⊥*Leiden Institute of Chemistry, Leiden University, P.O. Box 9502, 2300 RA Leiden, The Netherlands*

Received October 1, 2010; Revised Manuscript Received January 9, 2011

ABSTRACT: We present a multiscale modeling protocol to generate realistic amorphous polymer surfaces. Our computational approach consists of several steps having different levels of molecular detail. Initially, we generate a course-grained polymer surface that is completely relaxed using mesoscopic simulation methods. In the second step we transform the equilibrated coarse-grained polymer surface to atomistic detail with a special "mapper" that takes as input the mesoscopic morphology and uses Monte Carlo techniques to generate the atomistic structure. In the final step the atomistically detailed surface is equilibrated by performing a short molecular dynamics simulation. The great advantage of this multiscale approach is that it allows the study of compounds that have intrinsically (very) slow equilibration dynamics such as polymers, which would be difficult to study with conventional simulation methods only. In addition, the multiscale approach makes it straightforward to "move" between different levels of molecular detail and even zoom in on a relevant part of the mesoscopic structure and map only that part. As test cases we applied the multiscale modeling protocol to polyethylene, polypropylene, and polyacrylonitrile.

1. Introduction

The computational study of polymers is a challenging subject as the molecular weight can be large, excessing several hundred thousand monomers, depending on the type of polymer. In addition, the polydispersity of the polymer matrix can be high, making the modeling difficult as one has to generate a large number of polymer chains all with different lengths. In the 1990s Mattice and co-workers published a series of papers that focused on atomistic simulations of a number of simple polymer model surfaces of polyethylene (PE), polypropylene (PP), and poly(1,4-*cis*-butadiene) .[1−3] Using a relatively simple technique in which they extended the simulation box in one dimension, they were able to compute surface energies in line with experiment.

Multiscale modeling approaches at the particle level were first used in the early 1990s when quantum mechanics was coupled with molecular mechanics (QM/MM). For an overview of QM/MM see the work of Gao.[4] A typical example would be the study of an enzymatic reaction. The relatively small center of the enzyme would be treated at the quantum level, since there the reaction and/or conformational changes will take place, whereas the rest of the enzyme structure is described by a force field. In this way one is able to study relatively large systems at different levels of theory.

In recent years the number of papers that deal with multiscale modeling at the coarse-grained level has increased steadily. One can make a distinction between techniques that perform multiscale simulation on the fly or the ones that perform several steps in a row at different levels of coarse-graining, similar to the work presented here. In the former case simulations can have multiple spatial and time domains treated at different levels of coarse-graining, here termed collectively as hybrid methods. Similar to QM/MM methods, the difficulty with these hybrid methods is usually the overlap region, where the different spatial and time domains overlap, exchanging particles via sophisticated mapping techniques. Often this overlap region needs some additional parametrization. In the latter case the different coarse-grained spatial domains are strictly separated, and the mapping occurs in-between the simulation steps at different levels of coarse-graining, i.e., a so-called multiscale protocol. Although hybrid schemes with multiple coarse-grained domains are very appealing as only one simulation needs to be performed, they are hampered by the often difficult parametrization of the overlap region and have currently only been applied to relatively simple condensed phase systems. Some examples of the hybrid methods are the mesoscopic reactive scheme of Kapral and co-workers[5] and the adaptive resolution schemes of Kremer et al.[6,7] and Ensing et al.[8]

In two recent papers we demonstrated that by using the multiscale protocol approach, we could go from the atomistic, via the mesoscale level, all the way to finite element simulations .[9,10] Following the work of Müller-Plathe and co-workers,[11] we present an alternative simulation protocol that performs first a fast, coarse-grained simulation to equilibrate the polymer chain, then we perform a "mapping" to atomistic level, and finally we do a very short atomistic simulation. This work is organized as follows: First we describe the different steps of the simulation protocol, and then we give the results where we compare computed polymer properties against experimental results. We will end with some conclusions.

2. Computational Details

The simulation protocol to generate the bulk and surface polymer structures consists of three consecutive steps: (1) generate coarse-grained polymer structure; (2) mapping from coarse-grained to atomistic level, (3) equilibrate generated atomistic polymer structure.

Step 1 was done by performing a dissipative particle dynamics (DPD)[12,13] simulation using a $4 \times 4 \times 4$ cubic box. The box was

*To whom correspondence should be addressed. E-mail: janwillem.handgraaf@culgi.com.

Published on Web 01/26/2011

filled with soft-core particles (P) up to a density of 3.0, i.e., 192 particles. For the polymer surfaces, in the z-dimension a single-particle layer (W) was attached to the box. The positions of the W particles were fixed during the simulation. In the following all parameters related to the DPD simulations are given in reduced units. Temperature was set to 1.0, and the time step for the integration of the equation of motion was set to 0.015. The mapping factor was set to three, which means that every soft-core particle equals three heavy atoms. Using a mapping factor of 3 allows for sufficient molecular detail in the mesoscopic model of the polymer chains as we have the possibility to add polymer specific harmonic bond and angle terms. Using a density of 3.0, the repulsive a_{PP} interaction was set to 78.0. The DPD σ and γ were set to 3.0 and 4.5 following the standard work of Groot and Warren .[14] The P−W parameter was set to 156.0 in order to make the layer repulsive and thus impenetrable. At given intervals a bond was formed between two P particles to create a polymer chain until no single particles were left in the simulation box. In this way *one* polymer chain was "grown" in a solution of monomers. Bonds were described by harmonic springs. In addition, a harmonic angle term was turned on when the minimum number of particles in the chain was three. Equilibrium backbone bond lengths and angle values of polyethylene (PE), polypropylene (PP), and polyacrylonitrile (PAN) (see Table 1) were obtained from short-chain, single-molecule, molecular dynamics (MD) simulations using the OPLS all-atom force field .[15] Temperature was set to 300 K, and a time step of 0.5 fs was used. The total simulation time was 100 ps where we saved coordinates every 0.025 ps. Average bond and angle values were computed from the stored coordinates archive. The dihedral backbone value was also computed. However, it was found to vary substantially during a typical MD simulation, and hence, the dihedral term was not used in the mesoscopic simulations. k_b and k_a were set to 4.0 and 10.0, respectively. At the monomeric stage we performed 10 000 DPD time steps. After every bead addition to the growing chain the number of steps for an interval was increased in the following steps: 11 000, 12 000, 13 000, etc., until a maximum number of steps per time interval of 50 000. Once the complete chain was generated, an additional 500 000 steps were performed. At the final stage, to decrease bead−bead overlap, we set the harmonic bond spring constant to 40.0 and let the simulation run for another 50 000 steps. From the final run one snapshot was selected for the mapping step. In total, more than 8 million DPD steps were performed, which corresponds to 0.4 μs real time. For the mesoscopic model of bulk-phase polyethylene we checked the time invariance of the radius of gyration, R_g, and found it to be invariant at the final stage (see Figure 1 of the Supporting Information). In addition, the computed value for $\langle R_g^2 \rangle$ of 2.3×10^3 Å^2 is in the same order of magnitude as the value reported recently for bulk-phase polyethylene at 450 K obtained from MD simulations, i.e., $\approx 2 \times 10^3$ Å^2 .[11] While we are aware of the importance of entanglement effects[16] no attempt was made to include them in the current work as the chain lengths are relatively short. Note finally that for the generation of the bulk-phase mesoscopic polymer models we used exactly the same procedure as described above, apart from the fact that we did not use the repulsive wall.

In step two the mapping was performed from the soft-core mesoscopic to the atomistically detailed structures. First the repulsive wall was removed. In order to perform the mapping, we needed to define mapping relations; i.e., every soft-core particle represents an atomistic fragment or "blob". In Table 2 we collected the mapping relations for the different polymers, and Figure 1 shows the used fragments for polypropylene. In our case a typical soft-core polymer can be represented by the string H-(R_{190})-T. On the basis of the mapping relations given in Table 2, the atomistically detailed polymer structures were generated. In line with the mapping factor, the fragments contain three heavy atoms for PE and PP and four heavy atoms for PAN. As input of the mapping we set the densities to those of the bulk amorphous form of the polymer; i.e., ρ_{PE} = 0.834 g/cm^3 and ρ_{PP} = 0.869 g/cm^3 at T = 300 K, and ρ_{PAN} = 1.095 g/cm^3 at 400 K. In the case of PP and PAN the mapped polymer chains were isotactic. All atomistic models were described with the OPLS all-atom force field.[15] Long-range interactions

Table 1. Harmonic Bond and Angle Equilibrium Values Used in the Generation of the Mesoscopic Polymer Structures[a]

polymer	bond length (Å)	bond angle (deg)
PE	3.71 ± 0.28	140.8 ± 16.0
PP	2.59 ± 0.06	127.6 ± 22.7
PAN	2.62 ± 0.07	113.0 ± 15.1

[a] Values were obtained from single-molecule MD simulations of a short-chain polymer consisting of five repeat units.

Table 2. Relations for the Mapping from the Soft-Core Mesoscopic Polymer to the Corresponding Atomistic Polymer Structure[a]

soft-core particle	atomistic fragment ("blob")
H (PE)	$H_3C-CH_2-H_2C\cdot$
R (PE)	$\cdot CH_2-CH_2-H_2C\cdot$
H (PP)	$(CH_3)(CH_3)HC\cdot$
R (PP)	$\cdot CH_2-(CH_3)HC\cdot$
T (PP)	$\cdot CH_2-CH_2-CH_3$
H (PAN)	$(CH_3)(CN)HC\cdot$
R (PAN)	$\cdot CH_2-(CN)HC\cdot$
T (PAN)	$\cdot CH_2-CH_2(CN)$

[a] "H" denotes the "head" soft-core particle, "R" the "repeat" particle, and "T" the "tail" particle. Note that for polyethylene (PE) the head and tail particles are equal. Dots denote a bond connection point.

Figure 1. Atomistic fragments used for the mapping of polypropylene: (left) "head" fragment, (middle) "repeat" fragment, and (right) "tail" fragment. The blue ball-and-sticks indicate bond connection points.

were described with the Ewald implementation of Karasawa and Goddard[17] using a cutoff of 0.8 nm. An in-depth description of the mapping procedure is given in section 4 together with the results.

In the final step the mapped atomistic structures were allowed to relax using conventional molecular dynamics (MD) techniques. No prior energy minimization step was required. The velocity Verlet algorithm was used to integrate the equations of motion with a time step of 0.5 fs. For the bulk phase systems we performed 0.2 ns NPT simulations at $T = 300$ K for PE and PP and at $T = 400$ K for PAN using the Berendsen barostat[18] at ambient pressure. The average pressure was for all cases smaller than ±5 ATM. The standard deviation in the temperature and box edge was smaller than 1.5 and 0.5%. We performed several longer runs and found that the bulk-phase density remained constant. Furthermore, the results did not change if we performed an additional NVT run after the NPT run. For the surface models we extended the z-box dimension by 2.0 nm, creating a vacuum space. Initially, we placed two walls buildup of a lattice of argon crystal cells at the vacuum−surface interface. The system is depicted in Scheme 1. For the surface models NVT simulations were performed at $T = 300$ K for PE and PP and at $T = 400$ K for PAN using the Nose-Hoover thermostat.[19,20] The time step was set to 0.5 fs. Every 2000 time steps we measured the pressure exerted by the polymer phase on the two walls. As soon as the pressure was smaller than ±100 ATM on both walls the walls were removed from the simulation box. In most cases no more than 10 cycles were needed. The walls were used to make the simulation protocol more robust. After the mapping the density of the atomistic surfaces is homogeneous, whereas in the final equilibrated surface the density will drop at the polymer/vacuum interface. The walls ensured that the surface would not expand too much in the vacuum once the dynamics was turned on. A distance-dependent repulsion parameter in the DPD simulation might exclude the need to use these inert walls. We subsequently performed 1.0 ns NVT simulations without walls to further relax the polymer surface structures. Standard deviations in the temperature of the surface simulations were not larger than 10%. For both the bulk-phase and surface MD simulations we employed a cutoff of 0.9 nm for the long-range interactions. All calculations were performed with the Culgi software library.[21]

Scheme 1. Atomistic Surface Simulations[a]

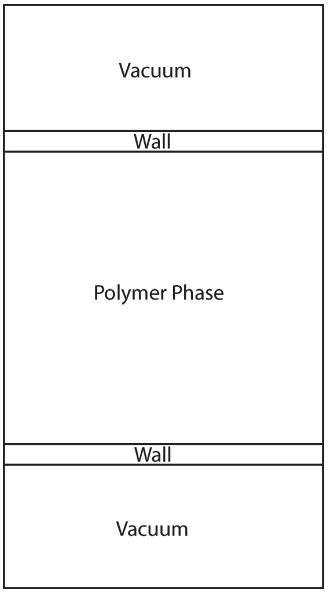

[a] The walls denote an one-atom layer thick lattice of "frozen" argon atoms.

3. Generation of Coarse-Grained Polymer Surface

Initially we performed a coarse-grained simulation using the dissipative particle dynamics (DPD) technique.[12,13] The DPD method is very well suited to fast equilibrate long polymer chains as it allows for simulation times up to seconds if needed. On the other hand, the DPD still allows for sufficient detail to make a distinction between, for example, polyethylene and polystyrene. In our case the coarse-grained polymer model is buildup of connected soft-core particles or "beads" where every bead is represented by three heavy atoms (see Figure 2).

We start with a solution of "monomer" beads, which we then "grow" bead by bead into a chain. This process is continued until there are no monomers left. You can envisage this process for example as a polymerization reaction that you perform in the lab. In this way one polymer chain was generated. Of course, the growth process could be stopped at a given chain length, and a new polymer chain could be formed. However, since our simulation box was rather small, we decided to have just one polymer chain. Connections between beads are based on the closest distance criterion. In the xy-plane of the simulation box we created a one-bead layer wall that is impenetrable by the monomers in solution. This wall ensures that the polymer "grows" only in two dimensions, thus creating a mesoscopic surface model. Figure 3 shows four snapshots of the simulation. To create a bulk-phase polymer structure, no wall was attached to the simulation, and hence the polymer chain was allowed to grow in three dimensions. To improve the resulting mesoscopic bulk and surface structure, we added harmonic bond and angle terms that were obtained from short-chain single molecule MD simulations of the respective polymer under study. For details of the bond and angle generation see section 2. At the final stage, after the equilibration

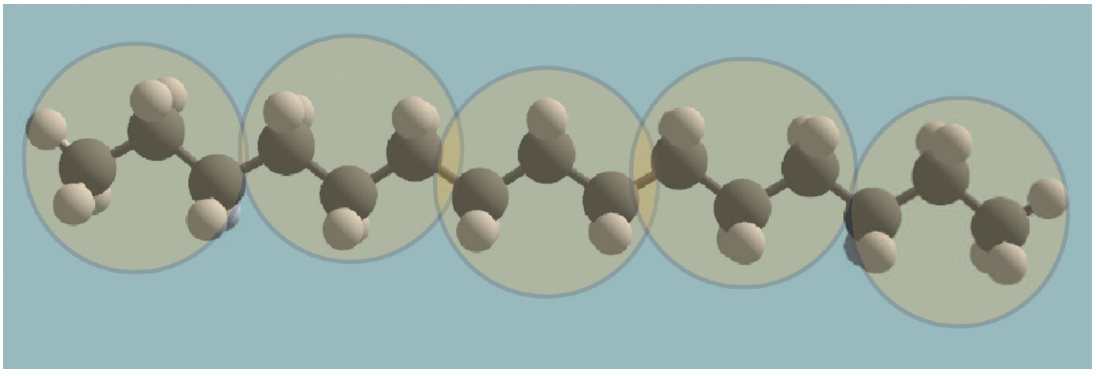

Figure 2. Coarse-grained model of a polyethylene polymer chain. Every soft-core particle represents three heavy atoms along the chain. Beads are connected by harmonic bond and angle terms.

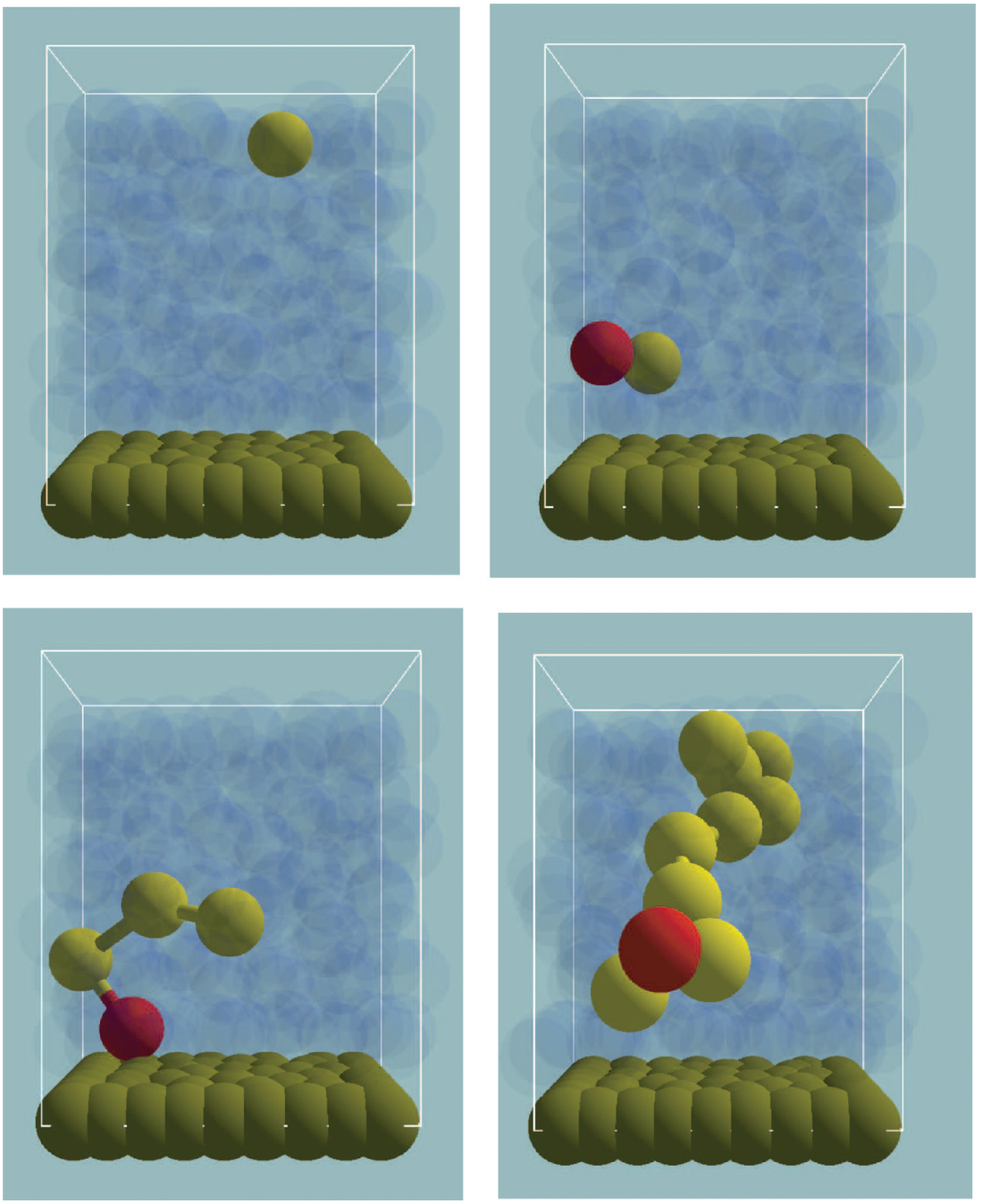

Figure 3. Snapshots of mesoscale simulation box where we grow a polymer chain in a solution of monomers. The polymer is allowed to freely grow in the *x*- and *y*-dimension and to a fixed extent in the *z*-dimension, as there is an impenetrable, stationary wall. Bead color coding: (red) polymer head bead from which the chain is growing; (yellow) polymer bead in chain; (brown); beads of wall. Monomers are visualized as opaque blue beads. From (left, top) to (right, bottom) the numbers of beads in polymer chain are 1, 2, 4, and 10. The polymer continues to grow until there are no monomers left in solution.

phase, the bead−bead harmonic constant was set to 40.0, making the bonds along the polymer chain rather stiff. We found that this improved the coarse-grained polymer structure used as input for the mapping step considerably. The overall simulation time was 0.4 μs, more than sufficient to allow for the polymer to completely equilibrate.

4. Mapping Coarse-Grained Structure to Atomistically Detailed Structure

Once a snapshot of the mesoscopic simulation was selected, we proceeded with the mapping step. The number density of the coarse-grained structure, usually 3.0, should be mapped to the desired density of the atomistic surface. A single bead in the coarse-grained model represents a fragment of a molecule, or "blob", in the atomistic model (see e.g. Figure 1). Information on the equilibrium local configuration of these molecular fragments is not available in the coarse-grained model. However, as the coarse-grained surface is well equilibrated, the goal of the mapping procedure is also to obtain an equilibrated structure. To ensure the desired density of the generated atomistic surface, we first calculate, and set, the size of the atomistic simulation box based on the amount of material to be placed in the box, independent of the size and density of the coarse-grained simulation box. Once the atomistic simulation box is created, the

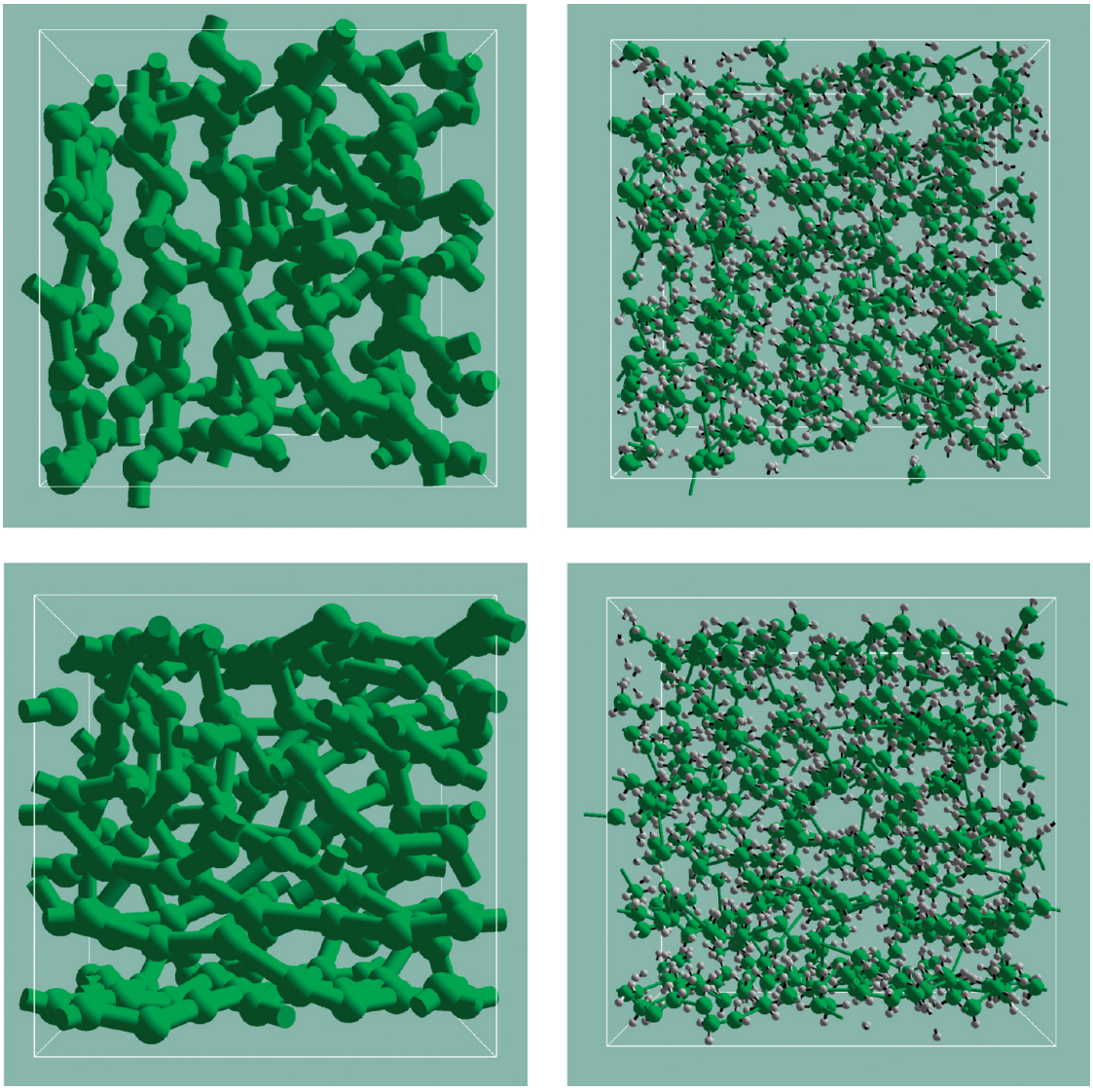

Figure 4. (top) Mapping of coarse-grained bulk-phase structure of PP to the corresponding atomistic structure. (bottom) Mapping of coarse-grained surface structure of PE to the corresponding atomistic structure after the stationary wall is removed. In both cases the coarse-grained structure contains 192 soft-core particles and the atomistic structure 1730 atoms.

mapping procedure generates the required number of molecular fragments with proper connectivity and morphology based on the coarse-grained structure. In mapping chain molecules each bead in the soft-core model corresponds to a single molecular fragment in the atomistic model. We now generate the desired molecular fragments for each bead in the system, identify the corresponding location of each soft-core bead in the atomistic simulation box by considering the dimension disparity between the boxes, and place each respective generated fragment in the atomistic box such that their centers fall on the corresponding locations of the beads. We also generate appropriate bonds to connect the fragments, following the connectivity information in the coarse-grained model. Note that the molecular fragments corresponding to each soft-core bead element type are identified a priori as part of the design of the coarse-grained structure, and thus the information regarding which atoms should be connected in replacing soft-core model bonds is well-defined. Since information on internal equilibrium configurations of each of the fragments in the atomistic structure is not known, we use vacuum-equilibrated configurations of individual fragments and place them at random orientations during mapping. It is clear that such an approach would generate structures with high intramolecular, such as bond stretching, bending, and torsion energies. Two separate measures are considered to improve on the local intramolecular structures of the generated molecules. The first is a premapping procedure that goes in the design of the coarse-grained system. Since all of the bonds and bending angles of the coarse-grained system directly transform to some corresponding bonds and angles in the atomistic structure, one needs to use appropriate bond stretching and angle bending constraints in the generation of the coarse-grained system. To this end, unlike common practice in DPD simulations, we use harmonic bond stretching and angle bending potentials in equilibrating our coarse-grained soft-core model surfaces as discussed in section 2. The second measure to improve the generated intramolecular structures of the atomistic surface is to perform random Monte Carlo procedures on the generated fragments. We employ two types of trial Monte Carlo moves: (1) rotational moves, where individual fragments are rotated around their own centers, and (2) stretch moves, where fragments are stretched or shrunk around their own centers. Both of the Monte Carlo moves are designed such that they do not affect the morphology of the structures, as present in the coarse-grained model. Note that the procedure to map from a soft-core mesoscale model to the corresponding

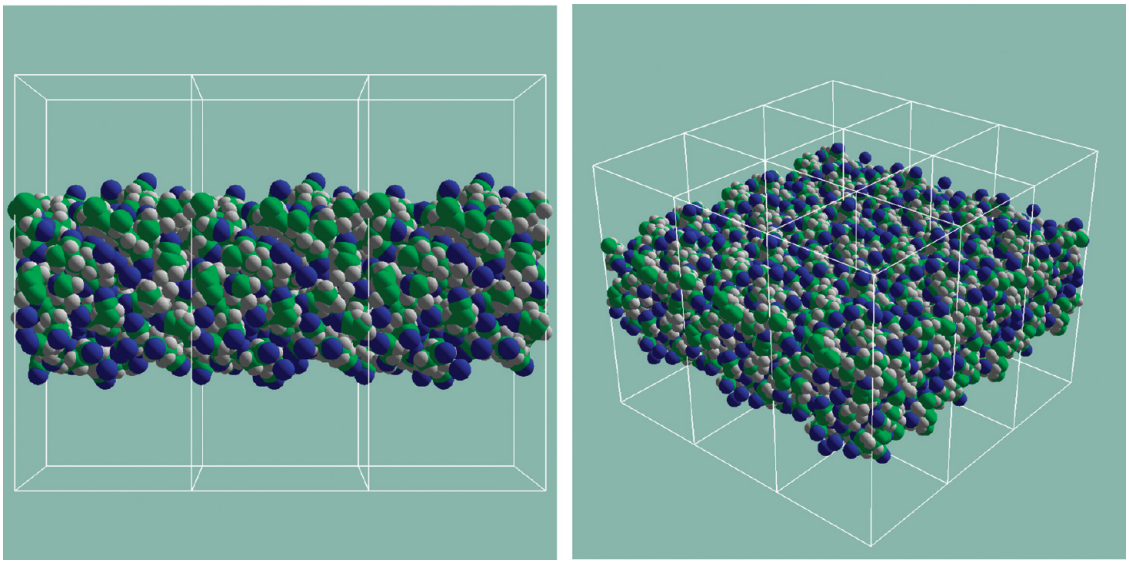

Figure 5. (left) Side view of polyacrylonitrile (PAN) atomistic surface model. (right) Top view of PAN atomistic surface model. The central simulation box is replicated once in the $-x$-, $-y$-, $+x$-, and $+y$-dimensions.

Table 3. Polymer Properties Obtained from the Amorphous Bulk and Surface Molecular Dynamics (MD) Simulations[a]

polymer	ρ (g/cm^3)	E_{coh}	δ_{tot}	δ_{disp}	δ_{elec}	$\langle\Delta E_{pot}\rangle$	$\langle\Delta E_{val}\rangle$	$\langle\Delta E_{disp}\rangle$	$\langle\Delta E_{elec}\rangle$	E_{surf}[b]	E_{surf}[c]	d_{surf} (Å)
PE	$0.834^{0.852}$	71 ± 1	$8.4^{8.0}$	8.4	0.3	75	−10	86	−2	33 ± 1	41^{33}	5.1
PP	$0.870^{0.855}$	62 ± 2	$7.9^{7.9}$	7.9	0.3	47	−59	98	8	30 ± 1	27^{29}	5.0
PAN	$1.095^{1.182}$	109 ± 3	$10.4^{12.2}$	7.3	7.5	97	−20	66	51	44 ± 1	54^{54}	4.6

[a] For polyethylene (PE) and polypropylene (PP) the data are at 300 K and for amorphous polyacrylonitrile (PAN) at 400 K. Error in the average bulk-phase densities are smaller than 0.01 g/cm^3. Cohesive energy densities are given in cal/cm^3, and solubility parameters (δ) are given in (cal/cm^3)$^{1/2}$. Energies are given in kcal/mol. $\langle\Delta E_{pot}\rangle$ is the averaged potential energy difference between the bulk and surface simulations. Similar definitions hold for the other energy terms where "val" denotes the valence terms (i.e. bond, angle, and torsion), "disp" denotes dispersion (van der Waals) interactions, and "elec" denotes electrostatics (Coulomb) interactions. Surface energies, E_{surf}, are given in dyn/cm. d_{surf} is the surface extension relative the bulk phase; see eq 5 for a definition. Where available, experimental values are given as superscripts. These values were for the most part taken from the work of Li and co-workers,[22] except for δ_{tot} (PE),[25] δ_{tot} (PP),[25] and E_{surf} (PP).[26] [b] Computed using eq 4; see main text. [c] Computed using eq 3; see main text.

atomistic model is completely integrated in the Culgi software library in a special mapper routine. It is possible that the generated atomistic structures may still contain some high intramolecular energy regions. In order to overcome this, we perform a few steps of MD simulation with small time step to improve on the local structures of the generated surfaces. Figure 4 shows as an example the mapping of a coarse-grained model of PP (bulk) and PE (surface) to the corresponding atomistic model. Note that for the coarse-grained and atomistic surface model no bonds cross the box edge in the $-z$- and $+z$-dimension.

5. Bulk and Surface Polymer Properties

Figure 5 shows a snapshot of the PAN surface as obtained from the MD trajectory. From the side view one can see that the surface is rather packed; i.e., only a limited number of molecular groups are actually protruding out of the surface. We will look in more detail at the atomic distribution, and in particular the orientation of the CN groups, of the PAN surface later on. In Table 3 we collected a range of physical and chemical properties of the three amorphous polymers under study. The simulations were run at 300 K for PE and PP and at 400 K for PAN. The surface simulation of PAN at 300 K did not converge due to the fact that the structure was most likely crystalline. This can be inferred from the relatively high glass phase transition temperature of PAN, i.e., 370 K.[22] The computed bulk phase densities are in excellent agreement with experiment. Note that for the bulk phase simulations 0.2 ns was sufficient to equilibrate the atomistic box, indicating that the mapped structure was already close to the final equilibrated structure. In addition, it shows that the coarse-grained model correctly describes the Kuhn length for the given polymer.

The Hildebrand solubility parameter[23] is defined as the square root of the cohesive energy density, E_{coh}, which in turn is defined as

$$E_{coh} = \frac{\Delta H_v - RT}{V_m} \tag{1}$$

where ΔH_v is the heat of vaporization, R the universal gas constant, T the temperature in kelvin, and V_m the molar volume. One can estimate ΔH_v from computer simulations using[24]

$$\Delta H_v = \langle E_{box} - \sum_{i=1}^{n} E_i \rangle - RT \tag{2}$$

where E_{box} is the (potential) energy of the simulation box, E_i is the energy of the individual molecules, and n is the number of molecules. The broken brackets indicate a time average over the length of the simulation. From Table 3 one can see that the computed value of PAN is underestimated by 20% compared to experiment. This could be attributed to the fact that we use a force field without polarization term. In a simulation it is straightforward to separate out the different energy terms. In Table 3 one sees that for PE and PP the electrostatic contribution to its solubility parameter, δ_{elec}, is negligible, whereas as expected, for PAN δ_{elec} takes up half of the solubility parameter. The length of the surface simulations after the mapping step is 1.0 ns. This is relatively short, considering that the surface needs to expand somewhat in the z-dimension to account for the decrease in density at the

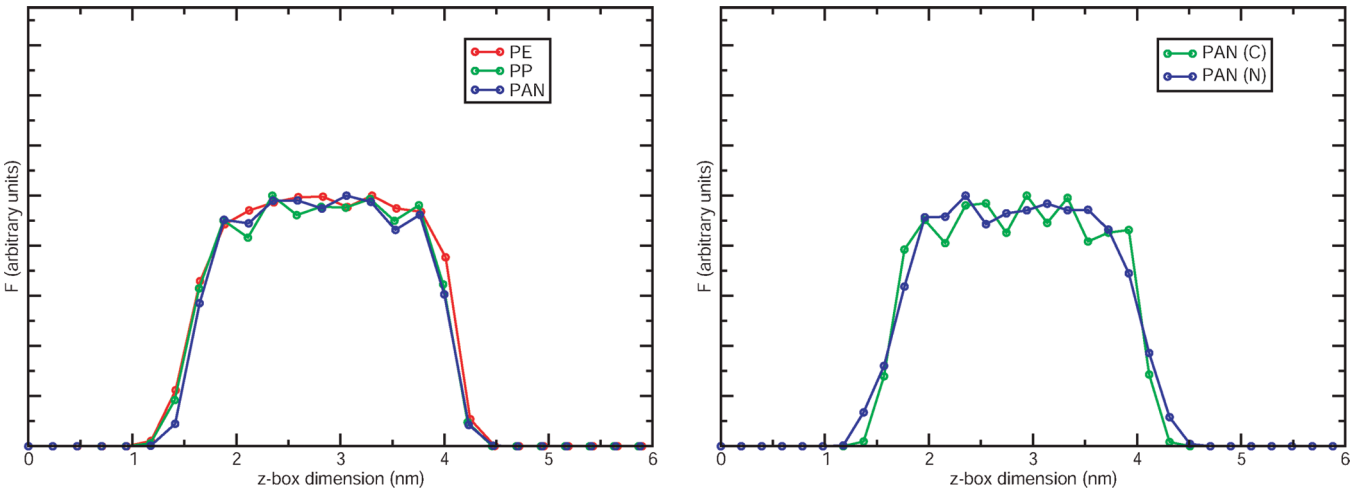

Figure 6. (left) Density profiles of the polymer surfaces across the z-box dimension. (right) Nitrogen and carbon density profiles of PAN surface. Profiles were generated from the polymer surface MD trajectories. Lines are just a guide to the eye.

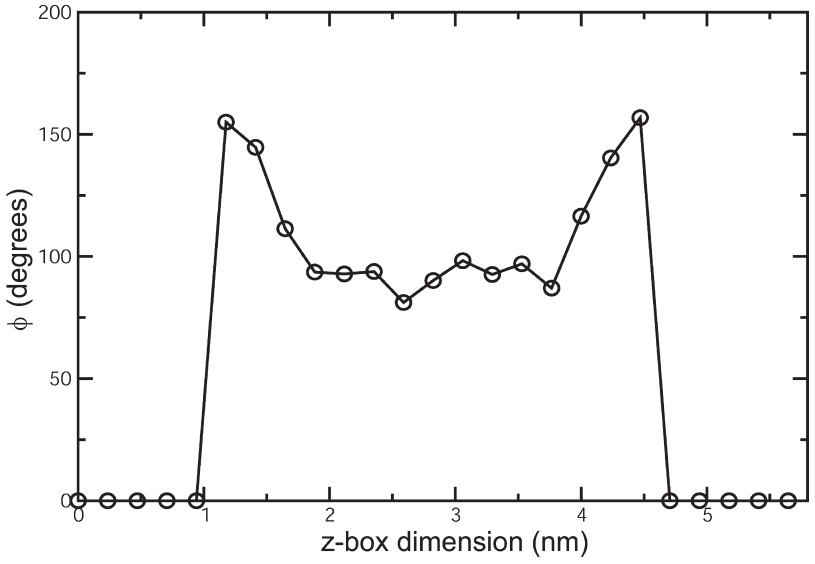

Figure 7. CN bond vector of PAN surface across the z-box dimension. Bond vector profile was generated from the PAN surface MD trajectory. Line is just a guide to the eye.

polymer/vacuum interface. Note that the mesoscale surface simulations were run at constant density. This means that at the start of the atomistic simulation the density at the interface is too high, and the surface needs to expand. We will come back to this point later on.

The surface free energy can be defined as[1−3]

$$E_{\text{surf}} = \frac{\langle E_{\text{bulk}}\rangle - \langle E_{\text{surf}}\rangle}{2A} \tag{3}$$

where E_{bulk} and E_{surf} are the bulk and surface free energy and A denotes the surface area at the polymer/vacuum interface. Similar to the work of Mattice et al.,[1−3] we neglect the entropic part of the free energy and simply use the potential energy. Again, the broken brackets indicate a time average over the length of the simulation. One can also estimate the surface energy directly from a bulk-phase simulation using

$$E_{\text{surf}} = (3/4)(E_{\text{coh}})^{2/3} \tag{4}$$

We want to stress that a comparison between this simulation work and experiment is difficult to make as there is a large uncertainty in the experimental values due to the large array of measurement techniques .[22] A further complication is that the temperature at which the measurements were performed is not reported in quite a number cases. Finally, there are small errors in the simulation methods that trace back to fitting of mesoscopic parameters from the atomistic simulations. Nevertheless, we want to make a comparison in order to see how accurate the applied multiscale protocol is. From Table 3 we see that the surface energies obtained using eq 3 match the experimental values quite well. For PAN the surface energy is exactly equal to the experimental value. This is likely fortuitous considering the uncertainties involved and probably points to some error cancellation but nontheless illustrates the ability of this protocol to construct realistic polymer surfaces and predict polymer properties. For PE the computed surface energies is somewhat too high compared to experiment. It difficult to understand what is causing this discrepancy as one can easily find literature values up to 40 dyn/cm. From Table 3 we see further that the surface energies using eq 4 are predicted very well for PE and PP and underestimated for PAN. This may suggest that more atomistic detail may be required in the mesoscale simulations for polymers with short polar side chains to predict highly accurate surface energies

or alternatively longer simulations may be required. An important point is that, even though the surface MD simulations were run for only 1.0 ns, already good to very good surface energies were obtained. This indicates that with a minimum of simulation time at the atomistic level we are able to get realistic polymer surfaces. Hence, most of the equilibration of the polymer chain takes place at the mesoscale level of theory.

If one splits out the potential energy change in valence, dispersion, and electrostatic contribution, it is evident from Table 3 that for surfaces the long-range interaction energy increases, whereas at the same time, the intramolecular energies decrease. This effect is especially pronounced for PP, most likely due to the rotational freedom of the methyl side group.

The surface extension is defined as follows:

$$d_{\mathrm{surf}} = l_{z,\mathrm{surf}} - \langle l_{z,\mathrm{bulk}} \rangle - d_{\mathrm{vac}} \quad (5)$$

where $l_{z,\mathrm{surf}}$ and $l_{z,\mathrm{bulk}}$ are the z-box dimensions of the surface and bulk simulations, respectively, and d_{vac} is the vacuum dimension. The surface extension indicates how much the surface structure will extend relative to the bulk- phase polymer. In Figure 6 we have plotted the polymer density profiles across the z-box dimension. The surface extensions of PE and PP are equal and 10% larger than d_{surf} of PAN. This indicates that PAN is more tightly packed than the hydrophobic PE and PP surfaces. For the PAN surface we computed in addition the density distribution of the carbon and nitrogen atoms (Figure 6 (right)). We find that on average the nitrogen atomic surface profile extends up 3.0 nm, whereas the carbon profile has a width of 2.8 nm. Hence, as was already evident from Figure 5, the CN groups stick out of the surface with the nitrogen atoms more exposed. In Figure 7 we have plotted the CN bond vector. If the vector is 180°, the CN bond lies exactly perpendicular to the surface interface. Clearly, this perpendicular ordering of CN side groups is highly favored close to the interface. This ordering gradually becomes less pronounced going toward the inner region of the surface where the surface has more bulk-phase character. All ordering is lost at 0.8 nm from the polymer/vacuum interface.

6. Conclusions

We have successfully applied a multiscale modeling protocol to generate realistic polymer surfaces of common polymers. Dissipative particle dynamics has been shown to be an accurate simulation method for fast equilibration of the polymer chains. In order to improve the mesoscopic polymer structure, we used a coarse-graining technique that included harmonic bond and angle terms from atomistic simulations in the description of the polymer chain. For the mapping of the polymer chain from mesoscale to atomistic level we used a technique that takes as input the coarse-grained particle positions and topology. From a collection of predefined molecular fragments ("blobs"), centered at the coarse-grained particle positions, an atomistic structure with the same topology is generated. Any overlaps between molecular fragments in this initial structure are minimized with Monte Carlo techniques. The input mesoscopic structure should not contain large residual particle−particle overlaps for the mapping to work properly, which is the reason we "freeze" the coarse-grained particles in space right before the mapping step. The final equilibration of the atomistic polymer structure using conventional molecular dynamics required only 0.2 ns for the bulk phase systems and 1 ns for the polymer surfaces. This short simulation time clearly shows that globally the atomistic structure was already close to equilibrium and that only locally molecular groups needed to reorient themselves. In principle, this multiscale modeling protocol could also be applied to (much) larger box sizes and more complicated amorphous materials including nanocomposites. At the mesoscale level one can add colloidal particles of any given shape and let them move via quaternion dynamics or keep them fixed in space. And within the mapping step there is the option to have more than two bonds per fragment; hence, dendrimeric and metal−organic framework structures[27] would be possible within the current implementation, with the obvious restriction that the force-field atom types are known and the material is amorphous in nature.

Overall, we find that for the multiscale modeling protocol to be successful the input coarse-grained structure should be "as accurate as possible". That is, it is necessary to set up a detailed coarse-grained model that gives a very good description of the atomistic structure. For these polymer systems dissipative particle dynamics (DPD) with additional bond and angle terms from atomistic simulations was sufficiently accurate. For more complex molecular systems one could think of additional intermediate mapping steps, such as the mapping from DPD to coarse-grained MD. The key thing is that the mapping steps should not involve too large molecular changes, so that sufficient molecular information can be transferred from one level of coarse-graining to the other.

In this work we verified the accuracy of the applied multiscale modeling protocol by comparing, besides standard bulk-phase properties, the computed polymer surface energies with experimental values, as we were specifically interested in surface energies for this study. In future studies we want to verify our multiscale protocol further by comparing polymer chain properties with literature data from polymer theory and experiment.

Supporting Information Available: A figure that shows the time invariance of the radius of gyration of bulk phase polyethylene as obtained from the mesoscopic simulation. This material is available free of charge via the Internet at http://pubs.acs.org.

References and Notes

(1) Misra, S.; Flemming, P. D., III; Mattice, W. L. *J. Comput.-Aided Mol. Des.* **1995**, *2*, 101–112.
(2) He, D.; Reneker, D. H.; Mattice, W. L. *Comp. Theor. Polym. Sci.* **1997**, *7*, 19–24.
(3) Natarajan, U.; Misra, S.; Mattice, W. L. *Comp. Theor. Polym. Sci.* **1998**, *8*, 323–329.
(4) Gao, J. *Rev. Comput. Chem.* **1996**, *7*, 119–185.
(5) Tucci, K.; Kapral, R. *J. Chem. Phys.* **2004**, *120*, 8262–8268.
(6) Praprotnik, M.; Delle Site, L.; Kremer, K. *J. Chem. Phys.* **2005**, *123*, 224106.
(7) Praprotnik, M.; Delle Site, L.; Kremer, K. *Phys. Rev. E* **2006**, *73*, 066701.
(8) Ensing, B.; Nielsen, S. O.; Moore, P. B.; Klein, M. L.; Parrinello, M. *J. Chem. Theory Comput.* **2007**, *3*, 1100–1105.
(9) Scocchi, G.; Posocco, P.; Handgraaf, J.-W.; Fraaije, J. G. E. M.; Fermeglia, M.; Pricl, S. *Chem. Eur. J.* **2009**, *15*, 7586–7592.
(10) Toth, R.; Voorn, D.-J.; Handgraaf, J.-W.; Fraaije, J. G. E. M.; Fermeglia, M.; Pricl, S.; Posocco, P. *Macromolecules* **2009**, *42*, 8260–8270.
(11) Carbone, P.; Karimi-Varzaneh, H. A.; Müller-Plathe, F. *Faraday Discuss.* **2010**, *144*, 25–42.
(12) Hoogerbrugge, P. J.; Koelman, J. M. V. A. *Europhys. Lett.* **1992**, *19*, 155–160.
(13) Español, P.; Warren, P. B. *Europhys. Lett.* **1995**, *30*, 191–196.
(14) Groot, R. D.; Warren, P. B. *J. Chem. Phys.* **1997**, *107*, 4423–4435.
(15) Jorgensen, W. L.; Maxwell, D. S.; Tirado-Rives, J. *J. Am. Chem. Soc.* **1996**, *118*, 11225–11236.
(16) Tzoumanekas, C.; Lahmar, F.; Rousseau, B.; Theodorou, D. N. *Macromolecules* **2009**, *42*, 7474–7484.
(17) Karasawa, N.; Goddard, W. A. *J. Phys. Chem.* **1989**, *93*, 7320–7327.
(18) Berendsen, H. J. C.; Postma, J. P. M.; van Gunsteren, W. F.; DiNola, A.; Haak, J. R. *J. Chem. Phys.* **1984**, *81*, 3684–3690.
(19) Nose, S. *Mol. Phys.* **1984**, *57*, 255–268.
(20) Hoover, W. G. *Phys. Rev. A* **1985**, *31*, 1695–1697.

(21) The Chemistry Unified Language Interface (Culgi), versions 3.0 and 4.0, Culgi B.V., The Netherlands, 2004−2010.
(22) Li, L.; Subu Mangipudi, V.; Tirrel, M.; Pocius, A. V. Direct Measurement of Surface and Interfacial Energies of Glassy Polymers and PDMS. In *Fundamentals of Tribology and Bridging the Gap Between the Macro- and Micro/Nanoscales*; Kluwer Academics Publishers: Dordrecht, The Netherlands, 2001.
(23) Hildebrand, J. H. *The Solubility of Non-Electrolytes*; Reinhold: New York, 1936.
(24) Belmares, M.; Blanco, M.; Goddard, W. A., III; Ross, R. B.; Caldwell, G.; Chou, S.-H.; Pham, J.; Olofson, P. M.; Thomasz, C. *J. Comput. Chem.* **2004**, *25*, 1814–1826.
(25) van Krevelen, D. W. *Properties of Polymers*, 3rd ed.; Elsevier: Amsterdam, 1990.
(26) Sauer, B. B.; Di Paolo, N. V. *J. Colloid Interface Sci.* **1991**, *144*, 527–537.
(27) Keskin, S.; Liu, J.; Rankin, R. B.; Johnson, J. K.; Sholl, D. S. *Ind. Eng. Chem. Res.* **2009**, *48*, 2355.